Winter Atmospheric Conditions over the Japan/East Sea

The Structure and Impact of Severe Cold-Air Outbreaks

BY CLIVE E. DORMAN, CARL A. FRIEHE, DJAMAL KHELIF, ALBERTO SCOTTI, JAMES EDSON, ROBERT C. BEARDSLEY, RICHARD LIMEBURNER, AND SHUYI S. CHEN

The Japan/East Sea is a marginal sea strategically placed between the world's largest land mass and the world's largest ocean. The Eurasian land mass extending to high latitudes generates several unique winter synoptic weather features, the most notable being the vast Siberian Anticyclone that covers much of the northeast Asian land mass. The Japan/East Sea's very distinctive winter conditions result from being on the east side of the Eurasian landmass at mid-latitudes. The resulting winter atmospheric conditions over the Sea include the mean cold air flowing off Siberia that is occasionally spiked with severe very-cold-air outbreaks.

In the winter of 1999–2000, a group of Russian, Korean, Japanese, and American scientists conducted an international program to investigate the oceanography of the Japan/East Sea and its surface forcing. During this program, we made atmospheric observations with a research aircraft and ships to understand the lower atmosphere and surface air-sea fluxes. We report here several highlights of these investigations with a focus on the dramatic severe cold-air outbreaks that occur three to five times a winter month. We start with a refresher on the physical setting and the winter mean and synoptic conditions, then describe the marine boundary layer and air-sea interaction based on research aircraft and ship measurements, and conclude with numerical model simulations that illustrate the special role of coastal topography on the surface wind field and air-sea fluxes over the Japan/East Sea.

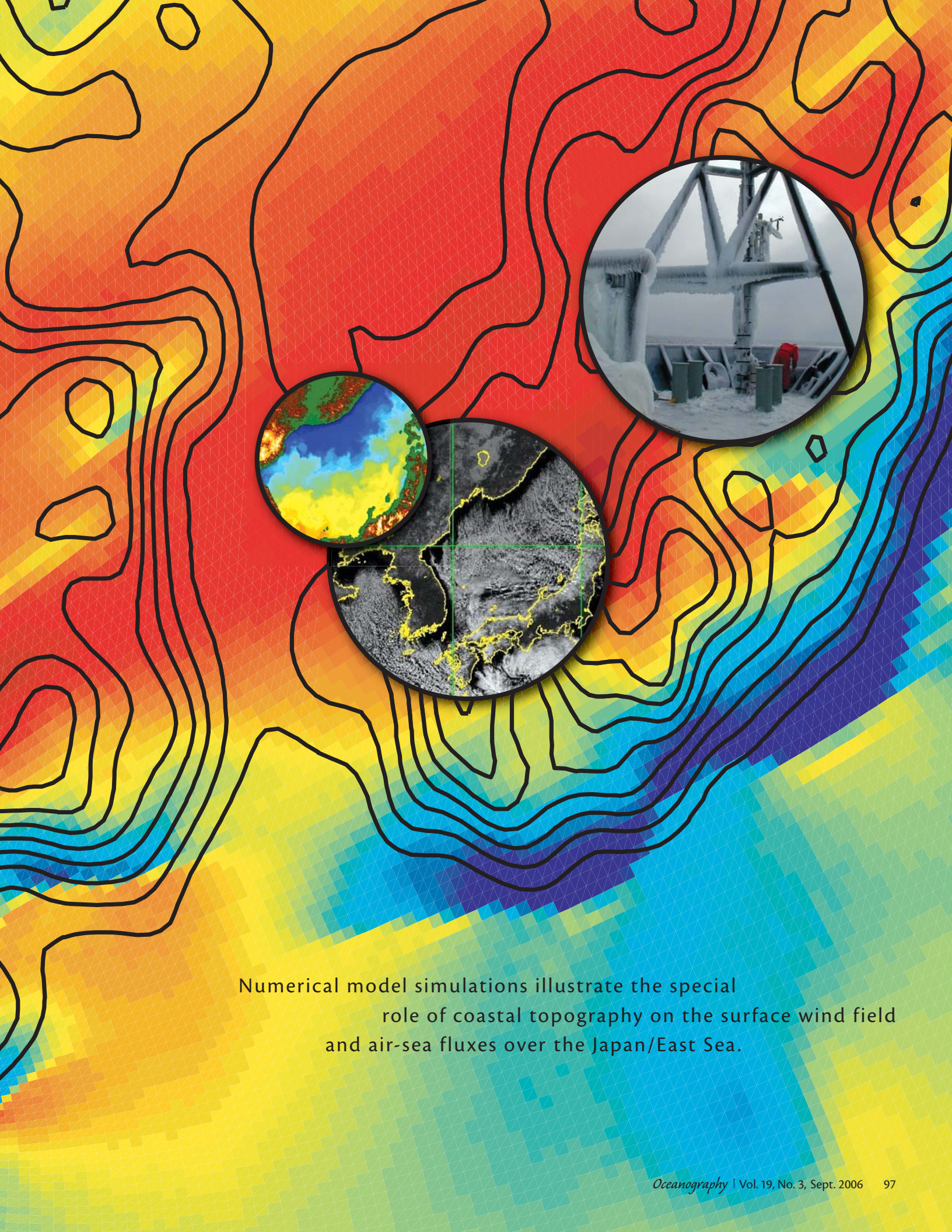

Numerical model simulations illustrate the special role of coastal topography on the surface wind field and air-sea fluxes over the Japan/East Sea.

PHYSICAL SETTING

The Japan/East Sea is surrounded by coastal mountains with peak elevations up to 2000–3000 m. Along the western side, the Sea is separated from the Manchurian Plain (average elevation ~ 300 m) and rest of the Eurasian continent by a coastal mountain range that runs uninterrupted from the Democratic People's Republic of Korea ("North Korea") to the Tatarskiy Strait, with the sole exception of the Vladivostok Gap (herein referred to as the Gap), a 200-km-long, 85-km-wide river valley that divides the Sikhote-Alin range to the northeast from the Hang-Yong mountains to the southwest (Figure 1). As we will see, cold Eurasian continental air masses have to overcome the obstacle represented by this coastal range in order to reach the Japan/East Sea. A shallow atmospheric boundary layer can only reach the Sea through the Gap, while a deeper layer capable of flowing over the mountain range will experience adiabatic compression (heating) as the air mass descends in the lee of the mountains, and thus will not be as cold as the ones that can reach the Japan/East Sea unhindered through the Gap. As a result, a combination of the surface topography, atmospheric stratification, and Earth's rotation can create strong local effects on the structure and flow of air in the marine boundary layer over the Japan/East Sea.

GENERAL WINTER CONDITIONS

The Japan/East Sea winter climatology is controlled by two large-scale features, the Siberian Anticyclone (High) centered near 100°E, 50°N and the Aleutian Cyclone (Low) in the Gulf of Alaska, which result in surface isobars oriented nominally north-south over the Japan/East Sea. In the middle atmosphere, a broad trough of low pressure is generally centered over the latitude of eastern Japan and is a portion of the largest amplitude stationary wave on the globe. The resulting mean winter condition is that cold air moving over the eastern Asian continent then moves over the Japan/East Sea, producing mean surface winds over the central Japan/East Sea from

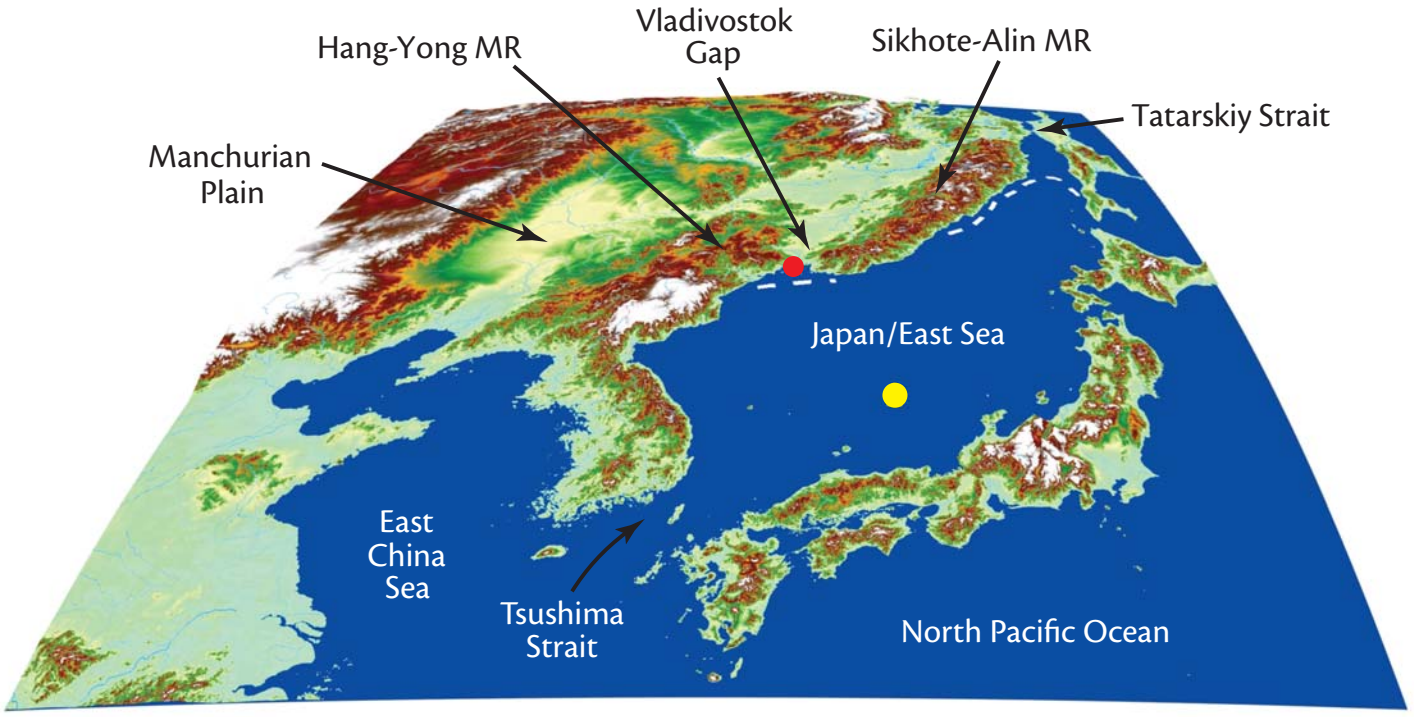

Figure 1. The Japan/East Sea, connecting waters, and surrounding lands. The land topography is shown on Earth's curved surface with a vertical exaggeration of 30 to illustrate the Asian continental landform and high coastal mountain ranges along the Korean and Russian coasts bordering the Japan/East Sea. The locations of Vladivostok and Japan Meteorological Agency (JMA) weather buoy 21002 are denoted by the red and yellow dots, respectively, and the mean edge of the winter fast ice along the Russian coast by the white dashed lines off Vladivostok and north near the Tatarskiy Strait. Note that the Vladivostok Gap along the Razdol'naya River valley is the primary gap in the coastal mountain ranges connecting the Manchurian Plain and lower plateau to the Japan/East Sea.

the northwest.

The January mean surface-air temperatures are -20°C to -15°C inland and to the west, rising to around 0°C along the Russian coast. The large surface-air temperature gradient across the Russian coast is due to significant coastal mountain lee-side warming (i.e., when the air flowing down the down-wind (lee) side of the mountain warms due to adiabatic compression), because the dominant air flow direction is almost exclusively toward offshore. The location of the surface 0°C isotherm, used as an operational index of the severity of cold-air advection, is generally oriented east-west and lies north of the center of the Japan/East Sea. The coldest sea surface temperatures, near 0°C, are found along the Russian central and southern coast, including areas near Vladivostok (Figure 2). The extreme northeast portion of the Japan/East Sea above 47°N is generally ice-covered in winter, especially in the shallow water to the west of Sakhalin Island; ice is also found in the immediate vicinity of Vladivostok (Figure 1) (Yakunin, 1999). Over the rest of the Japan/East Sea, the mean sea surface temperature increases to the south, reaching a maximum in the Tsushima Strait.

This mean weather state is modified by alternating lows and highs moving through the region towards the northeast. In general, we found that the winter weather can be characterized by four basic types of synoptic-scale conditions: (A) the dominant flow of cold Asian air towards the southeast over the Japan/East Sea, (B) passage of a weak low towards the northeast over the southern Japan/East Sea with a cold-air outbreak towards a southerly direction on the backside of the low, (C) passage of a moderate low towards the northeast along the northwestern side of the Japan/East Sea, and (D) an occasional very cold Siberian air outbreak towards the south and southwest. Here we present dramatic examples of two of these four basic cases, the dominant flow of cold Asian air towards the southwest (type A) that occurred on February 3, 2000 and the very cold Siberian air outbreak (type D) that occurred on January 24–26, 2000.

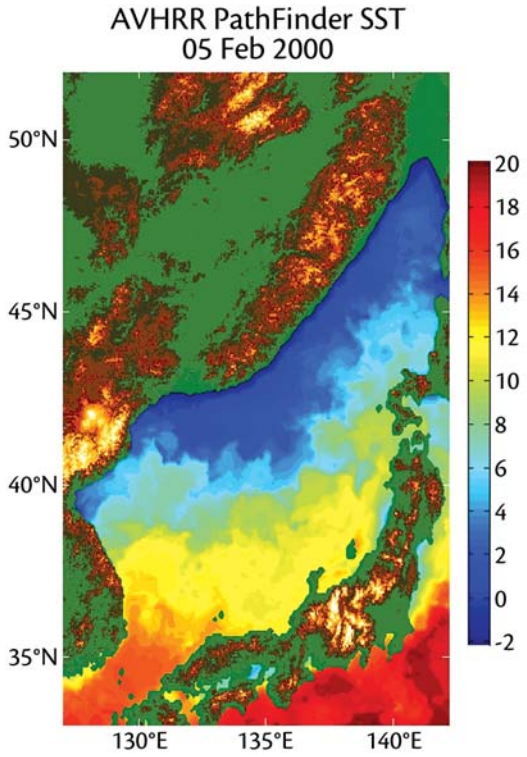

Figure 2. The Advanced Very High Resolution Radiometer (AVHRR) Pathfinder sea surface temperature (SST) (°C) 10-day composite centered on February 5, 2000 (which includes the period of the aircraft measurements shown later in Figure 6). The Subpolar Front, located near 40°N, separates the warm subtropical water entering the Japan/East Sea through the Tsushima Strait from the cold subarctic water to the north and northwest near Vladivostok during winter. The resulting strong SST gradient (of order 15°C) impacts weather systems by enhancing the surface pressure gradient and modifying the marine atmosphere boundary layer (Chen et al., 2001).

Cold Asian Air (CAA) Flow

Cold surface air originating from northern China passed over the Korean peninsula and eastern Russia and then over the Japan/East Sea on February 3, 2000,

Clive E. Dorman *(cdorman@ucsd.edu) is Research Oceanographer, Center for Coastal Studies, Scripps Institution of Oceanography, University of California, San Diego, La Jolla, CA, USA.* **Carl A. Friehe** *is Professor, Department of Mechanical and Aerospace Engineering, University of California, Irvine, Irvine, CA, USA.* **Djamal Khelif** *is Assistant Project Scientist, Department of Mechanical and Aerospace Engineering, University of California, Irvine, Irvine, CA, USA.* **Alberto Scotti** *is Assistant Professor, Department of Marine Sciences, University of North Carolina, Chapel Hill, NC, USA.* **James Edson** *is Professor, Department of Marine Sciences, University of Connecticut, Groton, CT, USA.* **Robert C. Beardsley** *is Scientist Emeritus, Department of Physical Oceanography, Woods Hole Oceanographic Institution, Woods Hole, MA, USA.* **Richard Limeburner** *is Senior Research Specialist, Department of Physical Oceanography, Woods Hole Oceanographic Institution, Woods Hole, MA, USA.* **Shuyi S. Chen** *is Associate Professor, Division of Meteorology and Physical Oceanography, Rosenstiel School of Marine and Atmospheric Science, University of Miami, Miami, FL, USA.*

where surface conditions were initially close to the mean January conditions. A high was centered over China. A low, located near the northeastern edge of the Japan/East Sea, moved east of northern Japan on February 4. Surface-air temperatures over northern China and eastern Russia were -15°C to -10°C. There was a rapid warming of surface air from -10°C near the Russian coastal mountaintops to -5°C over the Sea, due to lee-side subsidence and adiabatic warming. The 0°C surface-air temperature isotherm was located near 40–41°N in the center of the Japan/East Sea, slightly north of the January mean. The air temperatures were cold (-15°C to -20°C) and isothermal in the lower 1.5 km, testifying to the cold surface conditions and resulting strong stability of the lower atmosphere.

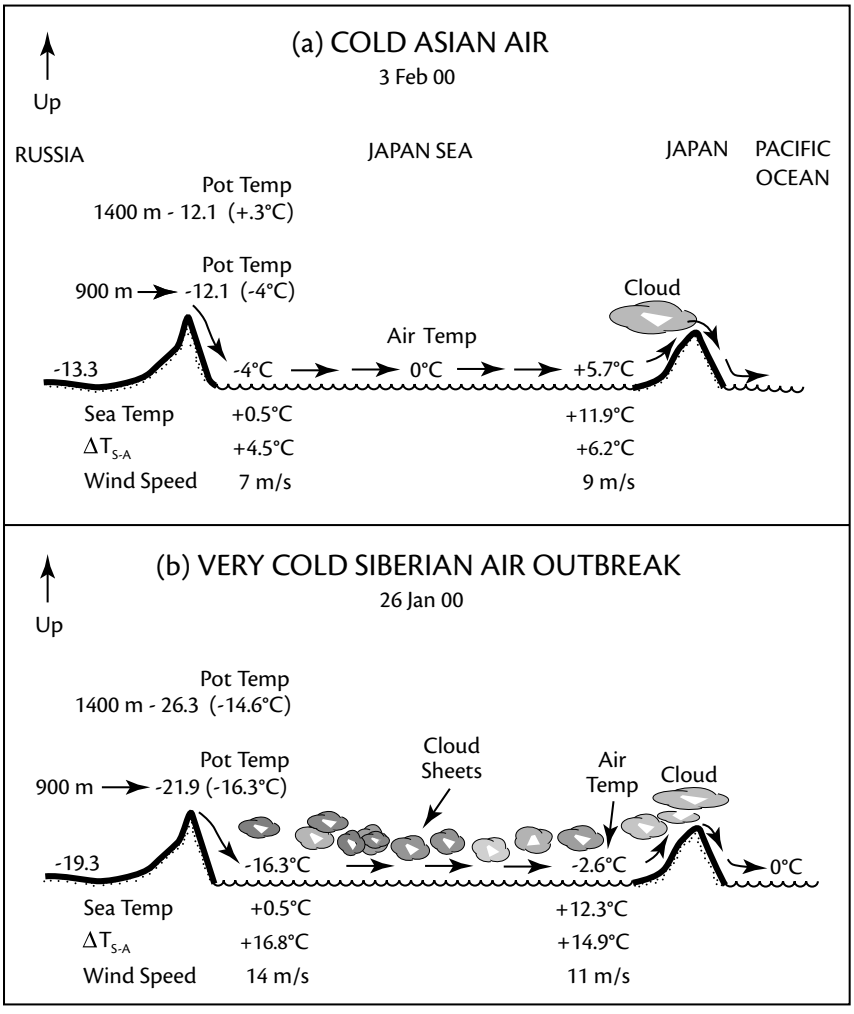

Figure 3. A schematic of the role of Russian coastal mountains in lee-side warming during (a) cold Asian air flow conditions and (b) a very cold Siberian air outbreak (VCSAO) moving over the Japan/East Sea. Both air temperature and potential air temperature in parentheses are given at 900 m and 1400 m to show vertical structure. Note the much lower surface-air temperature and larger sea-air temperature difference (ΔT_{S-A}) and wind speed during the VCSAO. Source: Dorman et al. (2004).

In Vladivostok, the surface air temperature varied between -15°C and -5°C, with the daily average about -10°C on February 3. The dry continental air kept the dew point 5°C to 10°C less than the surface-air temperature, and the sky was clear. The surface air in the center of the Japan/East Sea was considerably warmer, approximately 1°C to 4°C. The winds were toward the south at 5 m s^{-1}. The incident solar radiation was only modestly reduced by limited cloud cover. At the Japan Meteorological Agency (JMA) weather buoy 21002 on the southern side of the Japan/East Sea (Figure 1), the surface air temperature was about 5°C above freezing while the sea surface temperature was near 10°C. Thus, as the surface air moves from the Russian coast across the Japan/East Sea, the air warms up but remains cooler than the sea surface temperature. Figure 3a summarizes these February 3 conditions.

Very Cold Siberian Air Outbreak

The coldest and driest air moves over the Japan/East Sea as a severe Very Cold Siberian Air Outbreak (VCSAO), which occur on average three times per month in December or February and five times per month in January (Dorman et al., 2004). These very-cold-air outbreaks are formed in the Siberian High where January mean surface air temperatures can drop to -50°C and January mean daily minimum surface-air temperatures are near -60°C to -70°C. As mentioned above, cold air movement from the Russian interior to the Japan/East Sea is blocked to a degree by the coastal mountain ranges. Strategically placed lows can broadly advect air to the Japan/East Sea over the Russian coastal mountains.

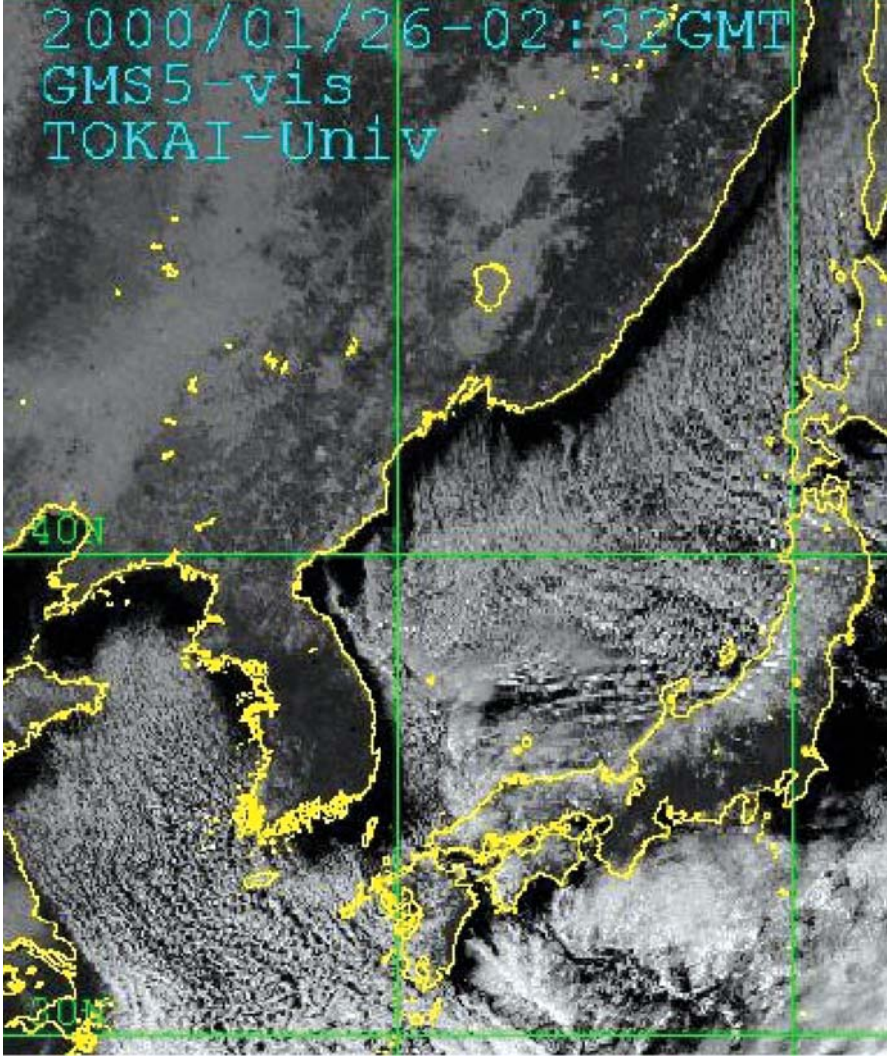

Figure 4. A Very Cold Siberian Air Outbreak (VCSAO) captured by a geostationary satellite visual image for 0232 UTC January 26, 2000. Cold, dry, cloudless Siberian air flows toward the south, across the coast, and over the Japan/East Sea. The narrow, clear zone on the north side of the Sea is where an atmospheric internal boundary layer is growing downwind from the coast but has not reached the height at which condensation will occur and clouds form. The large sea surface temperature minus air temperature difference causes strong vertical mixing in the atmospheric boundary layer, forcing air parcels to move in a long, helical path lined up with the mean surface wind streamlines. The upward motions generate the long cloud lines that form near the Russian and North Korean coasts, extending across the Sea to Japan. The result is a classical cloud sheet formed over this and other marginal seas, shelves, and ocean regions when very cold, dry continental air flows over open sea water. Source: Dorman et al. (2004).

These lows also force an intensified, low-level stream to the south through the Gap formed by the river valley headed by Vladivostok.

A classic VCSAO took place during January 24–26, 2000. On the 24th, the Siberian High moved south, resulting in NNE-SSW-oriented isobars over the Russian coast and the Japan/East Sea, initializing a strong, very-cold-air outbreak. The cold air flowing to the south over the Sea continued on the 25th and began to weaken on the 26th when the central pressure and aerial coverage of the Siberian High over the Japan/East Sea decreased.

Vladivostok soundings confirm that the air mass in the lower atmosphere during January 24–26 was much colder than the January mean (5°C to 12°C lower). Even more striking was that a strong ground-based inversion (i.e., a sharp transition between denser air normally found close to the ground and lighter air above) had been eliminated. As a result, the low-level stability was greatly reduced so that the potential temperature difference between 1000–850 hPa (roughly the lowest 1500 m of the air column) was small: only 5°C to 7°C. Winds exceeded 17 m s^{-1} towards the south at 800 m on all three days.

The 10-m air temperatures over the continent were coldest (-30°C to -20°C) on the 24th. On the 24th, the 0°C surface-air temperature isotherm had shifted to the center of the Japan/East Sea. On the 25th and 26th, this isotherm was in its southernmost excursion, extending from central Korea to mid-Honshu near 37°N. The 0°C surface-air temperature isotherm retreated to near 40°N on the 27th at the end of this strong, very-cold-air outbreak.

The surface air is modified as it moves southward across the Japan Sea on January 24–25. At Vladivostok, the air temperatures were -20°C to -18°C with clear skies and dry air. Arriving at the R/V *Revelle* near the center of the Sea, the air mass had been modified to -8°C to -0°C, with 10–13 m s^{-1} winds towards the south and marine cloud sheets. Passing over the southern edge of the Sea at the JMA weather buoy 21002, the surface marine air was near 0°C and 100 percent saturated, with winds towards the south at 10 m s^{-1} and cloud sheets.

Satellite visual images show sheet clouds filling the Japan/East Sea during very-cold-air events (e.g., Figure 4). Very strong vertical motions in the marine boundary layer are forced by cold air

pushing across warmer sea-surface water (House, 1993). The individual air parcels move in a long, helicial path, oriented with the mean wind direction and the vertical extent limited by the boundary layer thickness. The neighboring helixes are counter rotating so that a long, linear cloud forms under the rising air and a clear zone forms under the sinking air. Early in this VCSAO event on the 24th, there was a narrow clearing along the Russian coast, presumably due to the distance that the offshore air mass must travel before the large upward heat flux caused by the warmer sea temperature can overcome the lee-side subsidence. After this point, classical marine sheet clouds lined up with the surface wind.

We now consider why the air over the Russian coast away from Vladivostok is relatively warm during the dominantly occurring CAA flow conditions. The coldest inland surface air is blocked by the Russian coastal mountains. The reduced drag over the Sea in the lee allows acceleration and thus surface divergence, so that air from above the coastal ridge is pulled down in the lee of the coastal mountains, warming the coastal air to a temperature only 5°C to 10°C cooler than that of the sea surface (Figure 3). In contrast, during VCSAO events, both the surface and 1.5-km air temperatures over the Russian continental interior decrease to -20°C to -30°C, greatly reducing vertical stability and eliminating the surface inversion. The result is that during VCSAO events, the air originating from 500-m to 1000-m elevation inland moves over the Russian coastal range. Although the air is adiabatically warmed as it flows down to the ocean surface, it is still much colder than that observed during the more common CAA flow conditions.

Figure 5. Pilot Mike Hubbell in a survival suit preparing for a 10-hour research flight from the Misawa Naval Air Facility, Honshu, Japan. The five-hole radome wind on the nose of the aircraft system and some of the temperature and humidity sensors (under covers) around the radome are visible.

MARINE BOUNDARY LAYER STRUCTURE AND AIR-SEA FLUXES

As the cold Eurasian continental air moves across the generally warmer surface of the Japan/East Sea, the large air-sea temperature difference drives vigorous convection at the base of the marine boundary layer and enhanced air-sea fluxes. To investigate these boundary-layer processes, we used a special Twin Otter aircraft equipped to measure wind, temperature, dew point, pressure, sea-surface temperature, and the three components of the turbulent wind vector (temperature, and humidity to allow direct calculation of the horizontal momentum flux [wind stress] and sensible and latent heat fluxes by eddy covariance) (Figure 5) (Khelif et al., 2005). The sensible and latent heat fluxes represent the vertical turbulent transport of warmer, moister air from the ocean surface upwards into the atmosphere. The heat flux provides the buoyancy that carries this moist air upwards into the marine boundary layer. Condensation of this moist air is responsible for the cloud streaks shown in Figure 4 (i.e., these features are initially driven by air-sea exchange).

The aircraft, operated by the Center for Interdisciplinary Remote Aircraft Sensing (CIRPAS) of the Naval Postgraduate School, was based at the Misawa Naval Air Facility on the northeast tip of Honshu, Japan. To reach the region of high air-sea fluxes (the "flux center") located southeast of the Vladivostok

Gap (see insert Figure 6), additional fuel tanks were fitted for the ten-hour flights. Two types of flight patterns were flown: flux-center mapping and boundary-layer development. Flux-center mapping consisted of a grid pattern between 33-m altitude and the top of the boundary layer, while a downwind streamline "saw-tooth" pattern was flown to profile the developing marine boundary layer.

The growth of the marine boundary layer across the Japan/East Sea in cold Asian air flow and cold-air outbreak conditions is marked. Figure 6 illustrates this downstream change during the cold Asian air flow conditions on February 3 described above. A cold and dry high-speed wind issues from the Vladivostok Gap onto the relatively warm sea surface with ensuing vigorous air-sea interaction. The marine boundary layer, initially capped by a strong inversion at 400 m due to subsidence, immediately thins as it expands out over the Sea. Thereafter, boundary-layer growth due to strong turbulent mixing is roughly proportional to the square-root of the fetch, in qualitative agreement with simulations made with the U.S. Navy Coupled Ocean Atmosphere Mesoscale Prediction System (COAMPS). About halfway across the Sea, enough moisture has evaporated into the boundary layer that low-level clouds form. For clarity, Figure 6 shows only the progression of potential temperature profiles across the Sea. The air mass also becomes increasingly humid due to evaporation, and wind speed decreases due to momentum loss to the sea across the Japan/East Sea. Due to the mean southward increase in sea surface temperature (Figure 2), the air-sea temperature difference that partly drives air-sea heat exchange remains approximately constant across the Sea except near Honshu.

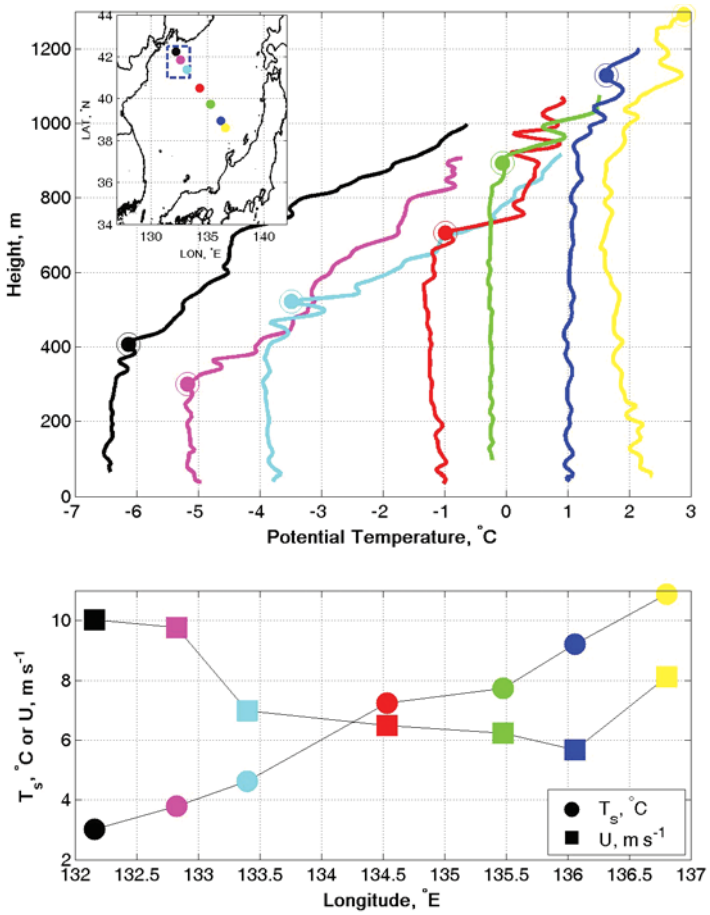

Figure 6. Top: Aircraft temperature soundings across the Japan/East Sea on February 3, 2000 during cold Asian air (CAA) flow conditions. The top of the internal boundary layer is indicated by the colored circle on each profile of potential temperature versus height; the map insert color-keys each profile to the location in the Sea and shows the location of the "flux center." Bottom: The decrease of surface wind speed (squares) and increase of surface temperature (circles) across the Sea as obtained at the bottom of each aircraft sounding. Note how the marine boundary layer initially thins then thickens crossing the Sea while the surface wind speed drops significantly at the southern edge of the "flux center" and continues to decrease across the Sea. Source: Khelif et al. (2005).

Our aircraft flux mapping patterns verified in general the concept of the high "flux center" advanced by Kawamura and Wu (1998). They used satellite sea surface temperature and scatterometer wind data with buoy measurements to estimate the winter surface wind stress and heat flux fields over the Japan/East Sea and found that these fluxes had local maxima (hence the name "flux center") in the area 41°N–42.5°N, 131.5°E–133.5°E where Japan Sea Proper Water (which fills the deep Japan/East Sea

below 200 m) is formed most winters (Sudo, 1986). Our maximum measured fluxes during severe cold-air outbreaks were 1 Pa for stress, 230 W m^{-2} for sensible heat and 190 W m^{-2} for latent heat. Total heat loss from the ocean (sensible and latent) varied from 100 to 400 W m^{-2} across the Sea from applying traditional bulk formula estimates to the aircraft data obtained at the bottom (33-m height) of the saw-tooth soundings. While stress decreased across the Sea from the "flux center," sensible and latent heat fluxes generally reached a minimum in the middle around 40°N, 135°E (south of the "flux center") and rose toward Honshu as the sea surface temperature increased from the mid-sea Subpolar Front south into the Tsushima Warm Current along the west coast of Japan.

The R/V *Revelle* also supported a suite of sensors capable of direct measurements of momentum, sensible heat, and latent heat fluxes. The sensor suite included a sonic anemometer to measure the turbulent wind vector and an infrared hygrometer to measure humidity fluctuations (Figure 7). During the outbreaks of cold Asian and very cold Siberian air over the relatively warm waters of the Japan/East Sea, the directly measured sensible and latent heat fluxes averaged 266 and 173 W m^{-2} during the January 25–27 VCSAO event and 135 and 156 W m^{-2} during the February 3 cold Asian air flow. The latter flux values are in good agreement with the aircraft measurements.

The R/V *Revelle* measurements also allowed us to measure directly the surface momentum flux (wind stress) under relatively extreme conditions. This momentum exchange drives oceanic waves and currents at the expense of some of the energy supplied by the heat fluxes. The momentum flux needs to be accurately parameterized in numerical models to predict accurately the circulation in both the ocean and atmosphere. For example, numerous investigations (and dimensional analysis) have shown that the exchange of momentum across the air-sea interface is proportional to the wind speed squared U^2. The flux is related to U^2 through a coefficient known as the drag coefficient, which depends on the roughness of the surface (i.e., the greater the roughness the larger the drag). Over the ocean, the roughness is provided by surface waves. Because the wave field is strongly determined by the wind field, it is not surprising that investigators have found that the drag coefficient itself is a function of wind speed. However, few investigations have been able to measure the drag coefficient (i.e., the flux divided by U^2) directly at

Figure 7. The extreme conditions driving the large fluxes over the Japan/East Sea often provide difficult operating conditions, as shown in this photo of the meteorological mast mounted on the bow of the R/V *Revelle*. Fortunately, the uppermost anemometers were deployed above the level of significant icing and operated during the majority of the cruise. The sonic anemometer is the device located above the two propeller-vane anemometers on the mast near the top of the photo. The infrared hygrometer was mounted next to the sonic (hidden by the mast in this photo).

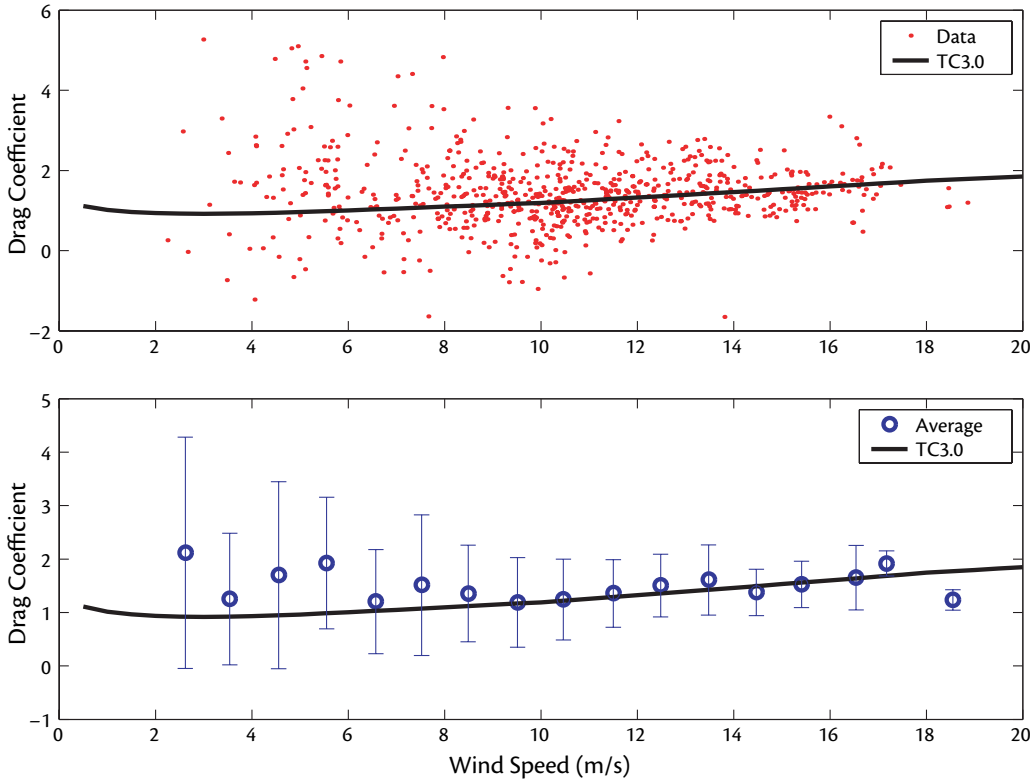

Figure 8. Top: Individual estimates of the drag coefficient (times 10^3) versus wind speed from the R/V *Revelle* flux system. Bottom: Values of the drag coefficients (times 10^3) averaged as a function of wind speed over 1 m s^{-1} bins. The error bars show the standard deviation about the bin-averaged means. The solid line in both panels is the TC3.0 prediction.

high winds. Our Japan/East Sea program provided such an opportunity as shown in Figure 8. The lower panel plot of bin-averaged drag coefficients versus wind speed exhibits good agreement with the latest bulk drag parameterization (the COARE 3.0 algorithm by Fairall et al., 2003) at wind speeds above 6 m s^{-1}.

Numerical modeling of the region provided additional details about the temporal and spatial variability of these fluxes in the region. For example, we conducted a two-month-long simulation (January–February 2000) using the Pennsylvania State University-National Center for Atmospheric Research Mesoscale Model (MM5) that allowed us to study the atmospheric forcing of various time scales from diurnal, synoptic, to monthly mean fields (Chen et al, 2001). The model shows that total surface fluxes can vary considerably over a short period, as illustrated in Figure 9 during the initial phase of the VCSAO on January 23–24. Topography has a strong influence due to the formation "jets" in the lee of the coastal range supports, a fact that is supported by the results of process oriented simulations described below.

A DYNAMICAL EXPLANATION

To investigate further the effects of the coastal mountain topography during cold-air outbreaks, we considered a shallow-layer model of the lower atmosphere and looked at two basic scenarios: the flow of a shallow surface layer discharging through the Vladivostok Gap, and the flow of a deeper surface layer able to overcome the coastal barrier (for details, see Scotti, 2005). Within these two basic scenarios we considered different combinations of initial and driving conditions. Before presenting results, it is helpful to consider qualitatively the main factors playing out during an outbreak. Under normal conditions, the pressure gradient aloft is directed to the south-southwest. At the same time, intense surface cooling over Eurasia creates a surface layer capped by a strong inversion. The shallow-water model is based on the assumption that this layer is thin (which allows us to neglect vertical accelerations) and free to slide frictionless under the layer above. The effects of the weather aloft are felt only through the pressure distribution at the upper boundary, while frictional effects with the topog-

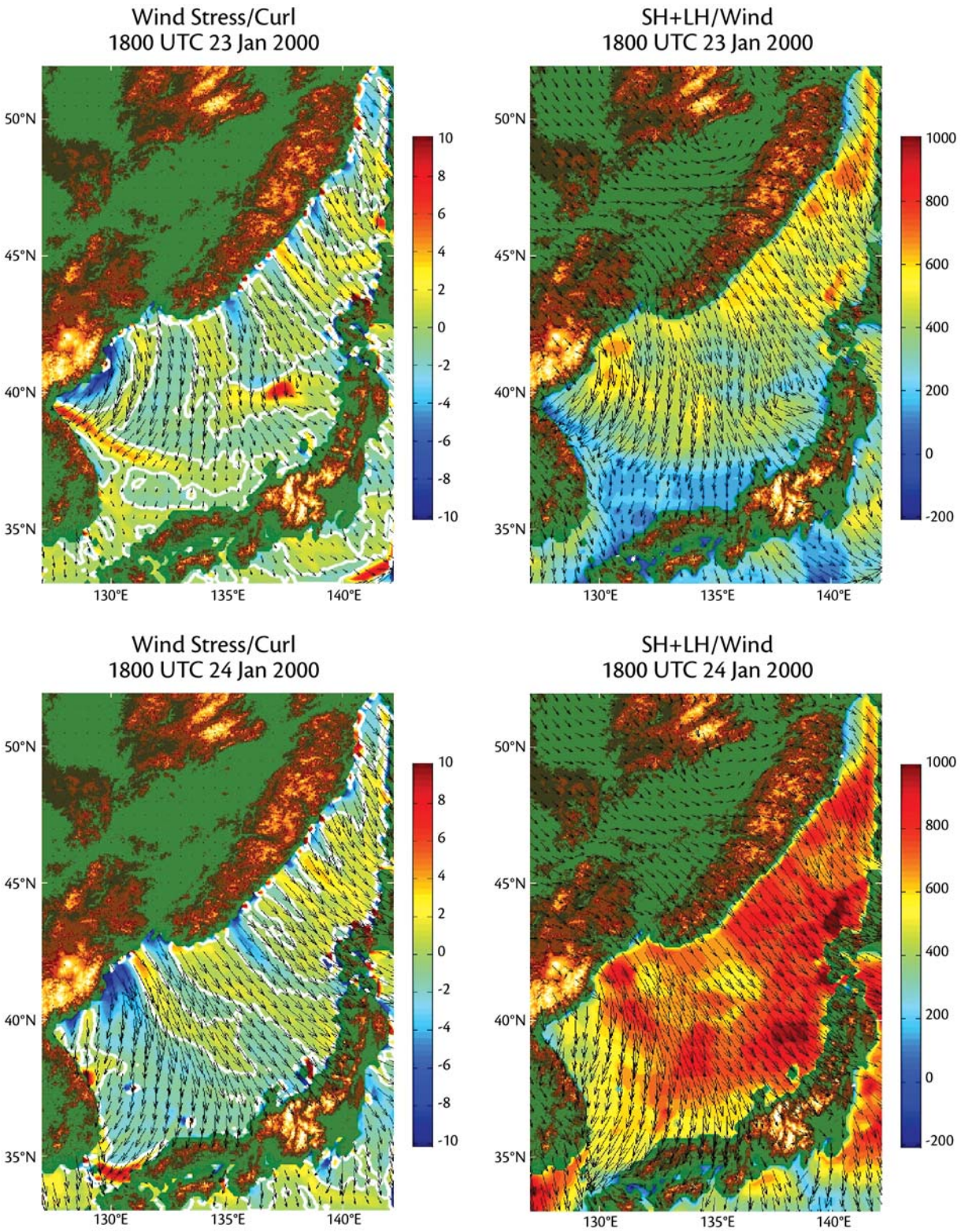

Figure 9. MM5 simulated surface wind stress (vectors in m s^{-1}) and curl (N m^{-3} x 10^{-6}, left panels) and surface air-sea heat flux (sensible and latent heat fluxes in W m^{-2}, right panels) during the initial phase (top panel-January 23 and bottom panel-January 24) of the Very Cold Siberian Air Outbreak that occurred January 24–26. Note the strong increase in wind stress and positive heat flux from the ocean into the atmosphere that occurs over this one-day period.

raphy underneath are represented with a simple quadratic drag law. If the layer is very shallow (first scenario), the layer along the Gap shallows from north to south, in balance with the pressure gradient aloft. If the layer is deeper (second scenario), the way it flows is controlled by the combined effect of geostrophy (due to Earth's rotation) and topographic control. During an outbreak, the pressure gradient aloft rotates in time towards the west. In the first scenario, the rotating pressure gradient acts as a gate swinging open, allowing the surface layer to accelerate down-channel. In the second scenario, the flow adjusts to the changing driving force by rotating to the south. The southward extending Gap, together with the peaks to the east and west of the Gap itself (Figure 10), create regions of locally intensified winds.

One robust result of our model simulations is that the first scenario considered is unlikely to generate a strong heat flux in the "flux center" southeast of Vladivostok, because the foothills of the Sikhote-Alin Range protruding into the Vladivostok valley floor force the flow to separate from the left (east) side of the channel and flow as a coastally trapped jet along the southwestern shore of the Japan/East Sea (Figure 11a, b). Counter-clockwise rotating eddies periodically form near the point where the flow detaches from the left wall of the channel and are advected by the flow downstream. In the second scenario (Figure 11c, d), the rotation of the pressure gradient aloft causes flow over the mountains that intensifies at the surface south of the Gap, over the "flux center." An interesting feature for this case is the existence of a very-well-developed wake in the lee of Gora Oblachnaya, and a less-developed one in the lee of Selin

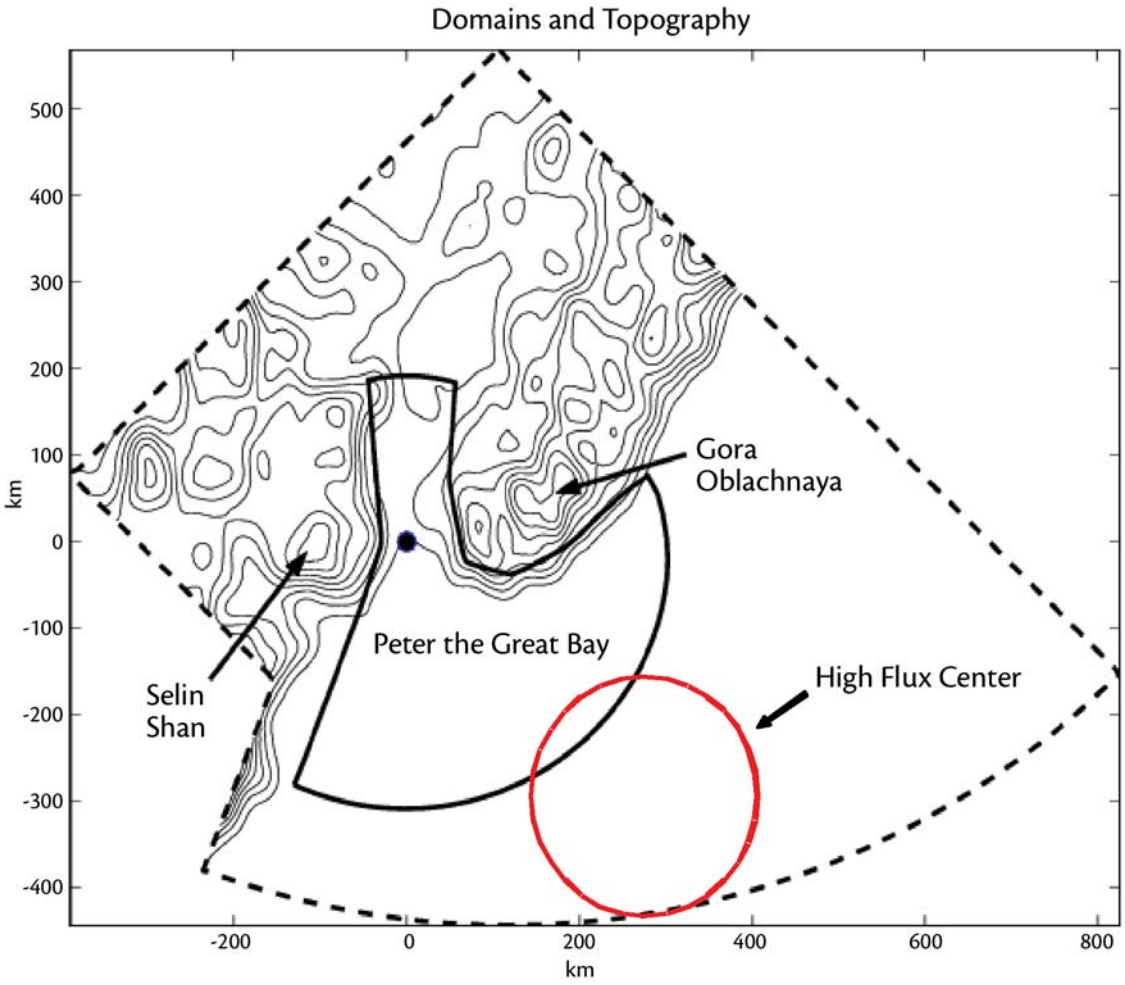

Figure 10. Domains used for the numerical simulations of a cold-air outbreak. The origin of the coordinate system is located in Vladivostok at the head of Peter the Great Bay. Shown are the locations of Gora Oblachnaya and Selin Shan, the two peaks that stand guard on either side of the Vladivostok Gap. Lines of constant elevation are spaced at intervals of 100 m. The solid line bounds the domain used to study the flow of a shallow lower layer flowing along the Gap, and roughly follows the 400-m elevation contour line (scenario 1). The broken line delimits the larger domain and topography used for the simulation of deeper lower layers overflowing the coastal mountain range (scenario 2). The approximate center location of the "flux center" is shown by the red circle. Source: Scotti (2005).

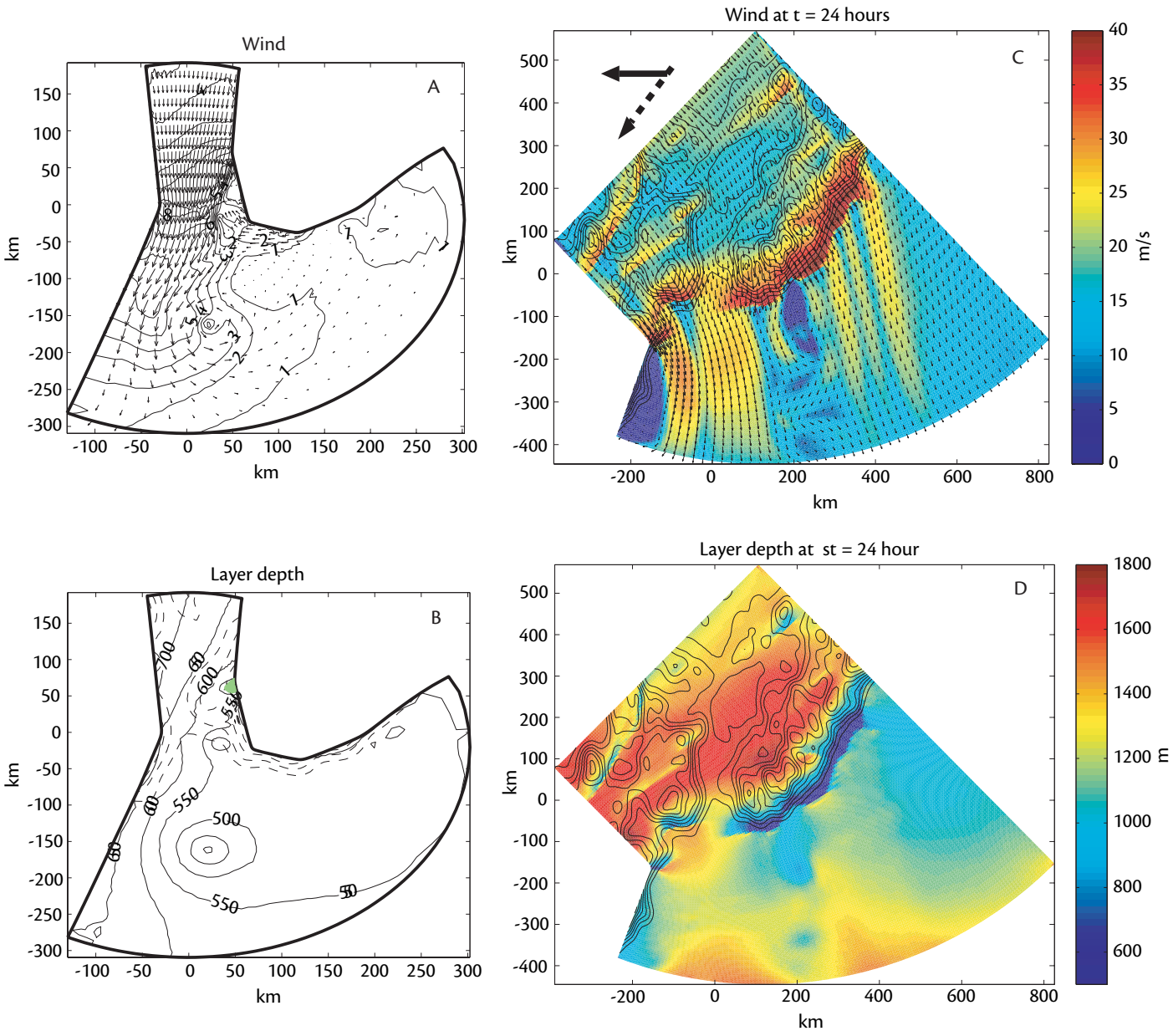

Figure 11. Left panels: a typical flow pattern for a layer constrained to follow the Gap, 32 hours after release (scenario 1). Panel A shows wind vectors and wind intensities, Panel B the layer depth (solid lines) and height of the topography along the channel (dashed lines). The effect of the hills protruding from the east (looking south down-channel) is to force the flow, which otherwise would fan rather symmetrically over the ocean, to detach from the east side of the channel and issue from the Gap as a coastally trapped jet. Periodically, counterclockwise eddies detach near the area where the flow separates and move downstream. Experiments with different initial conditions and forcing show similar patterns. Right panels: winds during a cold-air outbreak simulation with a thick lower layer that can flow over the coastal mountains (scenario 2). At the beginning of the simulation, the pressure gradient aloft is directed to the southwest (broken arrow in Panel C). The gradient slowly rotates to the west (solid arrow) over a period of 12 hours. Panel C shows the wind field 24 hours after the beginning of the experiment (12 hours after the pressure gradient has rotated to the west). Winds are intensified as expected over the coastal mountain range. A region of intense winds in the lee of the Gap is also evident, bounded on either side by the wakes of the two major peaks Gora Oblachnaya and Selin Shan (locations are shown in previous figure). Smaller peaks in the Sikhote-Alin range break up the flow over the ocean in a series of smaller jets and wakes. Panel D shows the depth of the lower layer. Note how the layer forms a region of minimum depth over the "flux center." Source: Scotti (2005).

Shan (see Figure 10). The flow in between is intensified. Also, note that the model predicts a minimum in the layer depth in the proximity of the "flux center," as observed during some of the aircraft flights.

SUMMARY

The Japan/East Sea lies on the eastern side of the world's largest landmass between 40°N–50°N. On that landmass is one of the great cold-air sources the world, the winter Siberian High. The great story here is the role topography plays in controlling the winter conditions over the Japan/East Sea, especially in modulating the effects of the Siberian High.

The Russian coastal mountain barrier holds back the lower very cold Siberian air. Instead, the air descends in the lee of the mountains, adiabatically warming, and greatly reducing the sea-air temperature difference and the heat loss from the Sea. The mean winter conditions over the Sea are sufficiently mild that only a small minority of the Sea is ice covered. As the southbound air moves across the Sea, the sea-air temperature difference remains roughly constant, because the air temperature and the sea surface temperature increase at about the same rate towards the south, and the marine boundary layer thickness increases.

Occasionally, the Siberian High strengthens for a few days, pushing much colder air over the coastal mountain barrier so that much colder air reaches the sea surface. The heat loss from the Japan/East Sea is doubled, ice coats ships, and distinctive cold-air outbreak sheet clouds cover the entire Sea.

Vladivostok is located at the mouth (southern end) of the only major gap in the Russian coastal range. This gap allows a narrow river of cold air moving down this valley from the eastern Manchurian Plain to the Japan/East Sea, with consequences beyond what might be imagined. The valley topography funnels and guides this air toward the Sea. When passing though the mouth, hydraulic effects accelerate the air, forming sea-level jets over water. These persistent high-speed winds carrying very cold and dry air over the surface of the Sea south and east of Vladivostok extract large amounts of heat and water, forming the "flux center" where Japan Sea Proper Water is created through deep convection that sinks and fills the bottom of the Japan/East Sea.

ACKNOWLEDGEMENTS

Many individuals contributed to the results presented here. In particular, we want to thank the CIRPAS aircraft facility personnel, especially Dr. H. Jonsson, pilots M. Hubbell and J. Stairs and the ground crew; the captains, crews and support staff of the R/V *Revelle* and R/V *Khromov* for their help with the shipboard meteorological measurements; D. Aldan (Scripps Institution of Oceanography), J. Ware (Wood Hole Oceanographic Institution [WHOI]), and S. Faluotico (WHOI) for their help with the air-sea flux instrumentation and data acquisition on the R/V *Revelle*; and Dr. N. Dashko (Far Eastern State Technical Fisheries University), Dr. K. Cho (Tokai University), Dr. S. Varlamov (Kyushu University), Dr. R. Matsumoto (Tokai University), and Dr. E. Uraevsky (Far Eastern Regional Hydrometeorological Research Institute) for their significant help. Feedback from Dr. K. Brink (WHOI) and two anonymous reviewers helped clarify the final manuscript. Support for this component of the Japan/East Sea Departmental Research Initiative was provided by the U.S. Office of Naval Research (ONR). We want to especially thank Dr. S. Murray (ONR) for his considerable assistance and encouragement with this study.

REFERENCES

Chen, S.S., W. Zhao, J.E. Tenerelli, R.H. Evans, and V. Halliwell. 2001. Impact of the AVHRR Pathfinder sea surface temperature on atmospheric forcing in the Japan/East Sea. *Geophysical Research Letters* 28:4,539–4,542.

Dorman, C.E., R.C. Beardsley, N.A. Dashko, C.A. Friehe, D. Khelif, K. Cho, R. Limeburner, and S. M. Varlamov. 2004. Winter marine atmospheric conditions over the Japan/East Sea. *Journal of Geophysical Research* 109:1–26.

Fairall, C.W., E.F. Bradley, J.E. Hare, A.A. Grachev, and J.B. Edson. 2003. Bulk parameterization of air-sea fluxes: Updates and verification for the COARE algorithm. *Journal of Climate* 16:571–591.

House, R.A. 1993. *Cloud Dynamics*. Academic Press, San Diego, CA, 573 pp.

Kawamura, H., and P. Wu. 1998. Formation of Japan Sea Proper Water in the flux center off Vladivostok. *Journal of Geophysical Research* 103:21,611–21,622.

Khelif, D., C. Friehe, H. Jonsson, Q. Wang, and K. Rados. 2005. Wintertime boundary-layer structure and air-sea interaction over the Japan/East Sea. *Deep-Sea Research II* 52:1,525–1,546.

Scotti, A.D. 2005. Orographic effects during winter cold-air outbreaks over the Sea of Japan (East Sea): Results from a shallow-layer model. *Deep-Sea Research II* 52:1,705–1,725.

Sudo, H. 1986. A note on the Japan Sea Proper Water. *Progress in Oceanography* 17:313–336.

Yakunin, L.P. 1999. Ice drift and thickness in the Sea of Japan. In: *Proceedings of the Fourth CREAMS Workshop*, held February 1996. Far Eastern Regional Hydrometeorological Research Institute, Vladivostok, Russia.